Supporting Information for

Probing Surface Functionality on Amorphous Carbons using X-ray Photoelectron Spectroscopy of Bound Metal Ions

Andrew J. Carrier,[a] Inusa Abdullahi,[a] Barrie Fiolek,[b] Kelly A. M. Hawboldt,[c] and Stephanie L. MacQuarrie[a*]

[a]Department of Chemistry, Cape Breton University, 1250 Grand Lake Road, B1P 6L2, Sydney, Nova Scotia, Canada

[b]B. W. BioEnergy Inc., 1615 Grand Lake Road, B1M 1A3, Sydney, Nova Scotia, Canada

[c]Department of Process Engineering, Faculty of Engineering and Applied Sciences, Memorial University of Newfoundland, A1B 3X5, St. John's, Newfoundland and Labrador, Canada

S1.1 Pre-cleaning of biochar

The as-received biochar was dispensed into a 500 mL beaker and was soaked in deionized water. This mixture was heated to boiling with stirring and held at that temperature for 15 min. The granular carbon was filtered with a Whatman No. 40 filter paper using a Buchner funnel. The carbon was returned to the beaker and the

*Corresponding author. Tel: 1 (902) 563-1302. Fax: 1 (902) 563-1880. E-mail: stephanie_macquarrie@cbu.ca (Stephanie MacQuarrie)

washing process was repeated twice more until the filtrate ran clear and had no charred-wood odor. The clean granular carbon was dried in an oven at 100 ºC for 2 d. After this the carbon was placed in a blender and ground for 10 min before sieving to a ≥150 μm particle size.

S1.2 Acid-washing of biochar

A sub-sample of biochar prepared via the method in section S1.1 was measured into a 250 mL Erlenmeyer flask after which 0.1 M HNO_3 solution was added at a rate of ~125 mL/g. The mixture was gently swirled to ensure complete coverage of the biochar then allowed to sit undisturbed at ambient temperature for 24 h. At this point the solution was filtered, and a portion of the filtrate was reserved to measure any extracted ions. The filter cake was briefly rinsed with deionized water to remove residual acid then dried in an oven at 115 ºC. The resulting powder was scraped into a clean Erlenmeyer flask and the soaking process was repeated once more before drying and storing the material. Rinsing the carbon with deionized water removes any residual acidity as stirring the resultant carbon in deionized water generates a pH 7 solution.

S1.3 Non-linear Data Fitting and Discussion

The adsorption data (Figures S8–13) were used to determine Langmuir and Freundlich isotherm model constants that are summarized in Tables 3 and S5 (and

for activated carbon in Tables S6 and S7). The root mean square error (RMSE) was on the same order of magnitude for both the Langmuir and Freundlich isotherms, and the constants are compared against activated carbon and other published values. For the Freundlich isotherm the "1/n" value is referred to as adsorption intensity and reflects the type of sorption sites. When n=1 all sites are considered similar, n>1 reflects a heterogeneous surface and favourable adsorption. All metal ions exhibited n>1. The K value reflects the adsorption capacity. Cu^{2+}, Zn^{2+}, and Pb^{2+} showed the most favourable binding in the Freundlich model.

S1.4 Supplemental Tables and Figures

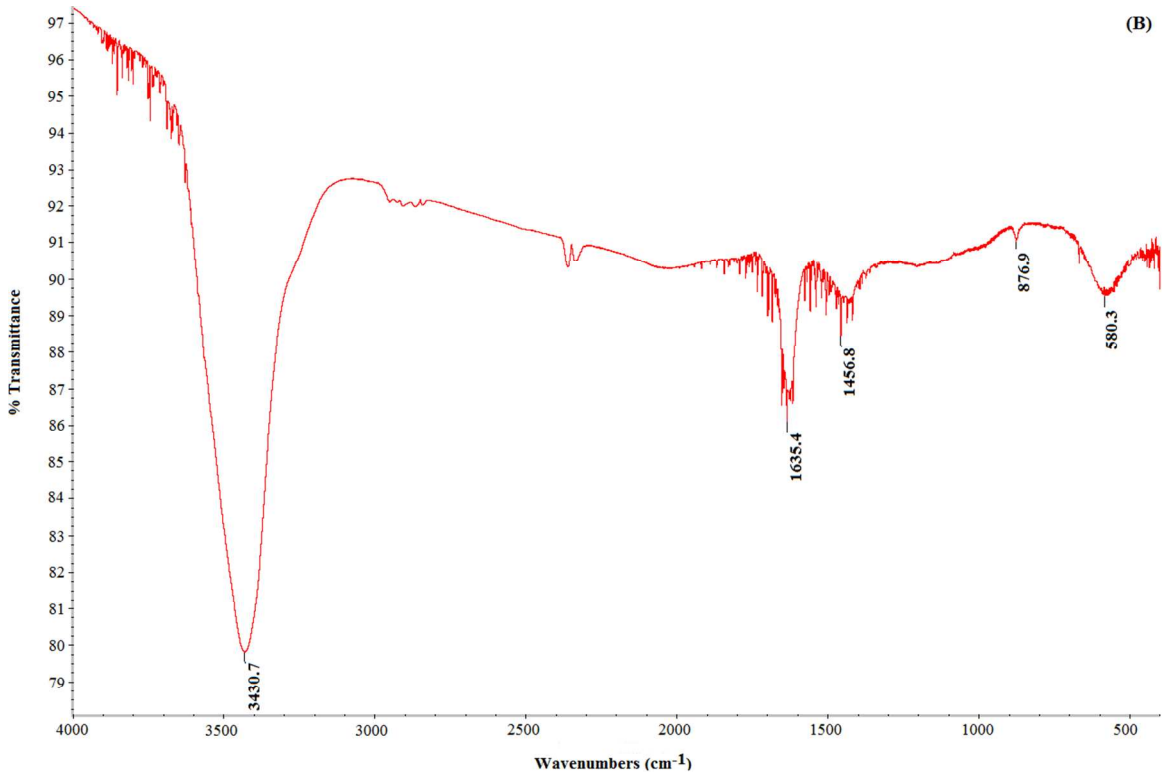

Figure S1. Fourier Transform-Infrared (FT-IR) spectra of birch biochar.

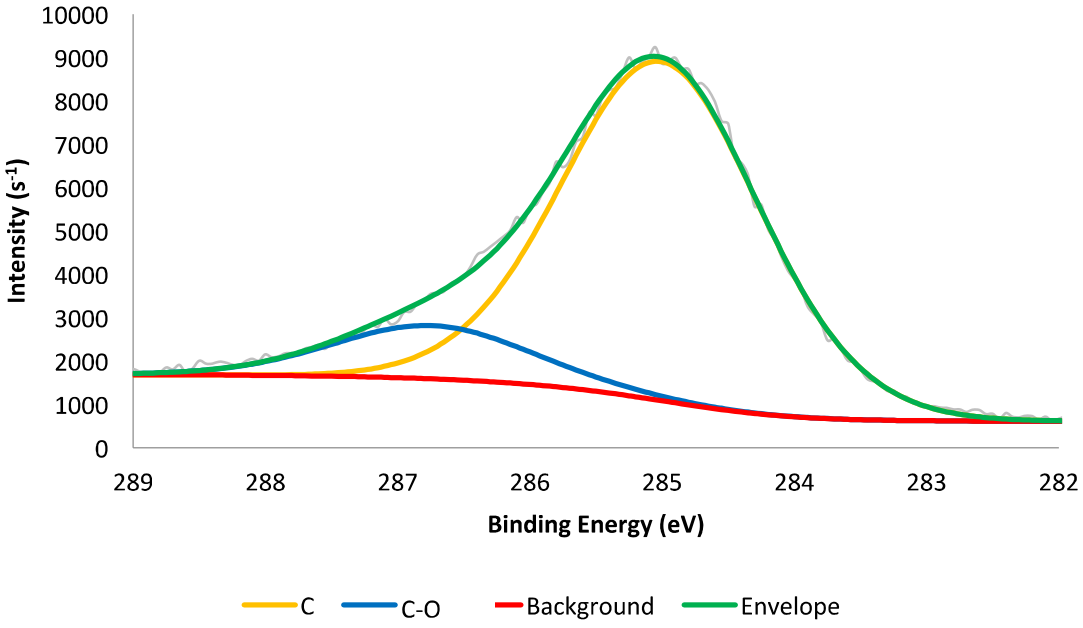
10000
9000
8000
7000
6000
5000
4000
3000
2000
1000
0
Intensity (s-1)
289
288
287
286
285
284
283
282
Binding Energy (eV)
C
C-O
Background
Envelope

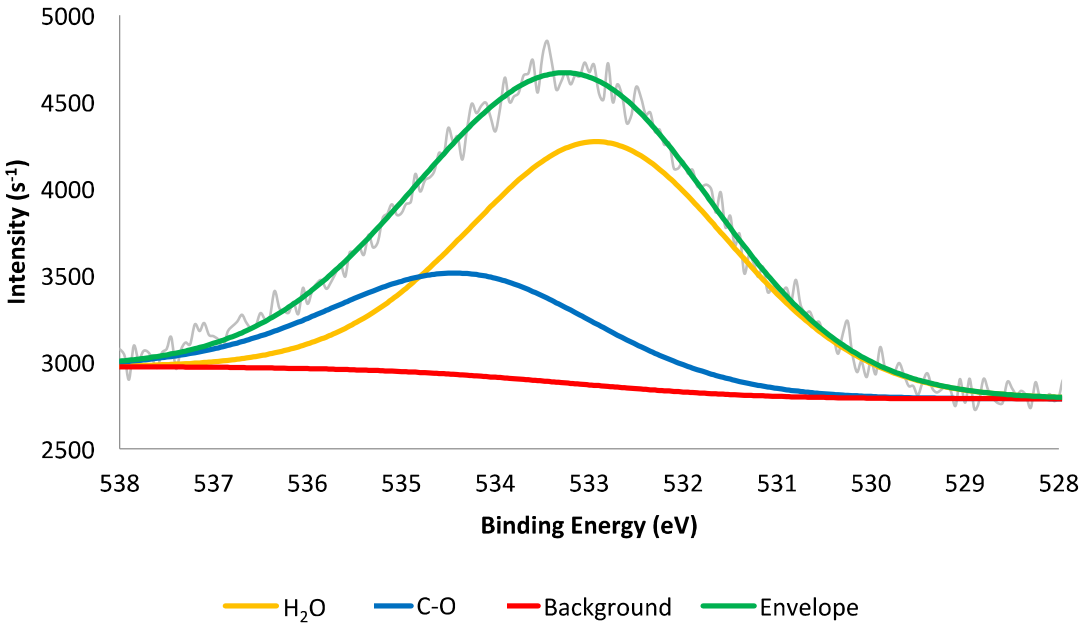
5000
4500
4000
3500
3000
2500
Intensity (s-1)
538
537
536
535
534
533
532
531
530
529
528
Binding Energy (eV)
H2O
C-O
Background
Envelope

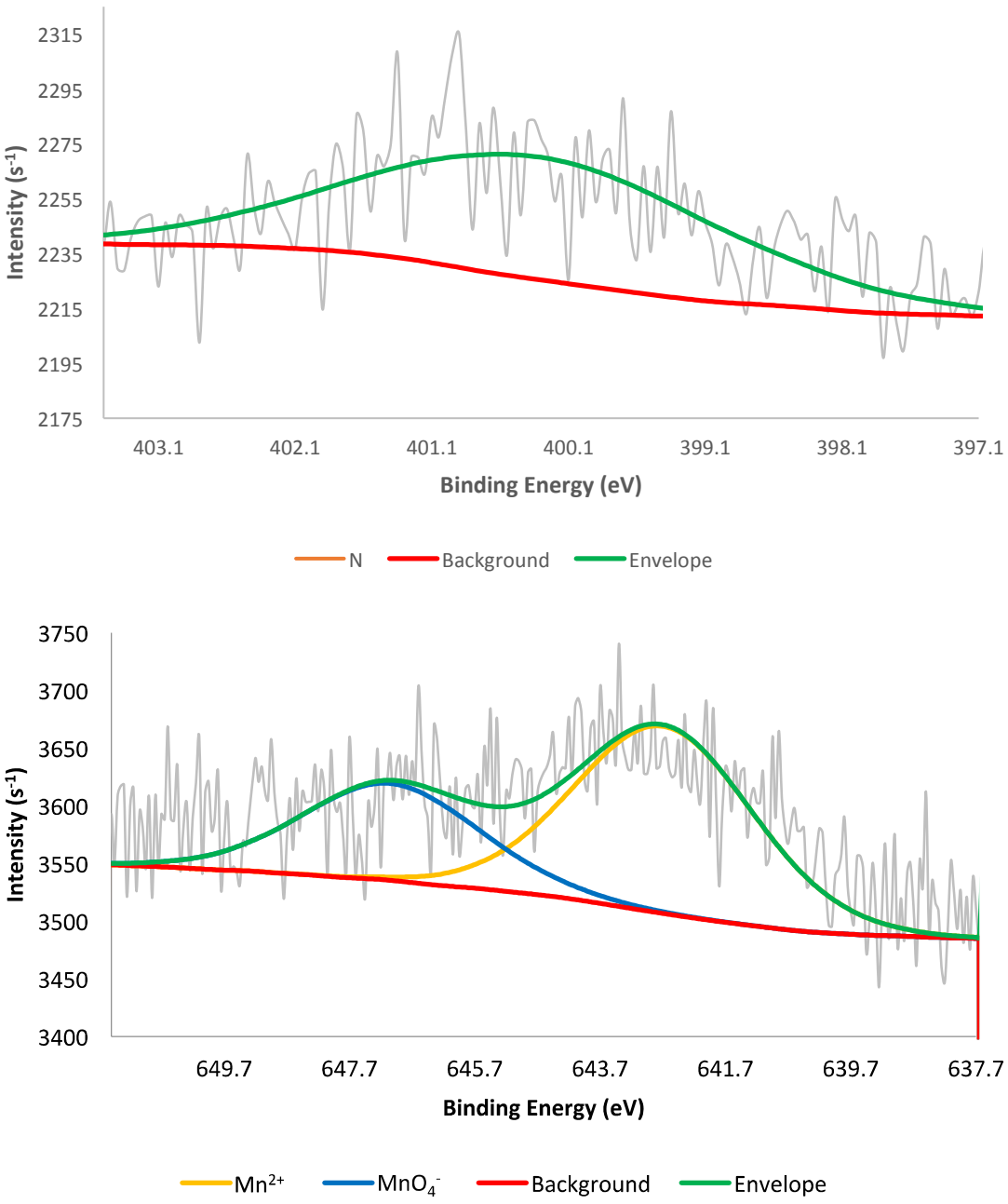

Figure S2. X-ray photoelectron spectra of the Mn-doped biochar. From top to bottom: C1s, O1s, N1s, and $Mn2p_{3/2}$.

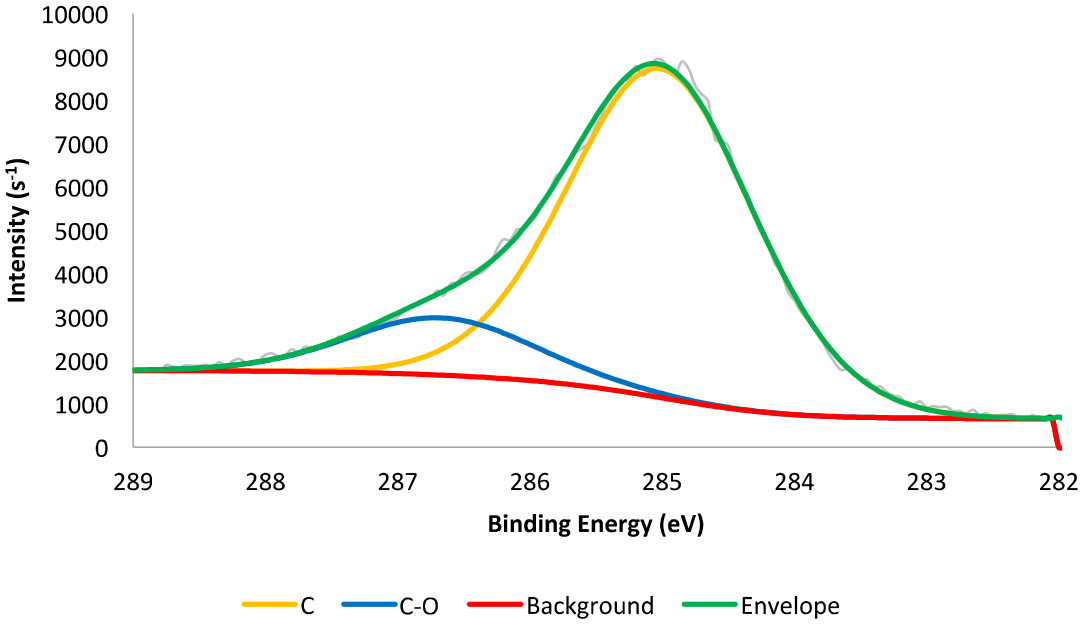
10000
9000
8000
7000
6000
5000
4000
3000
2000
1000
0
Intensity (s-1)
289
288
287
286
285
284
283
282
Binding Energy (eV)
C
C-O
Background
Envelope

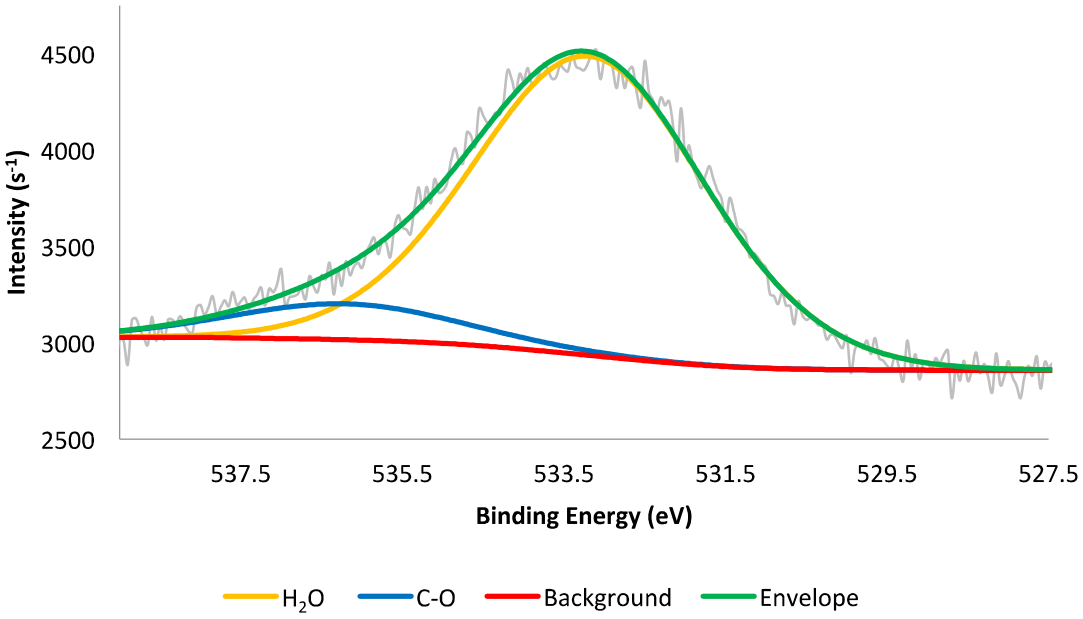
4500
4000
3500
3000
2500
Intensity (s-1)
537.5
535.5
533.5
531.5
529.5
527.5
Binding Energy (eV)
H2O
C-O
Background
Envelope

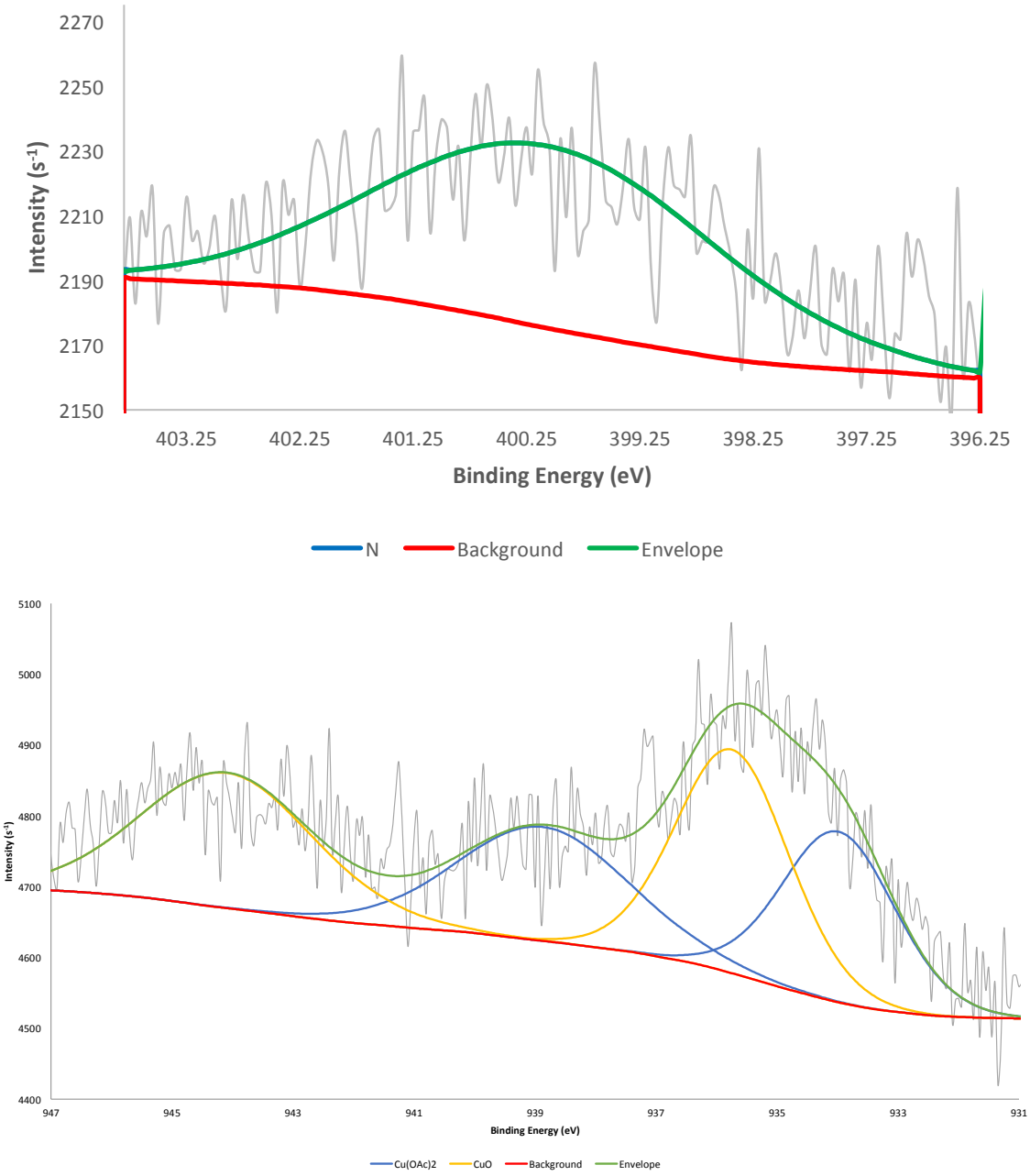

Figure S3. X-ray photoelectron spectra of the Cu-doped biochar. From top to bottom: C1s, O1s, N1s, and Cu2p$_{3/2}$.

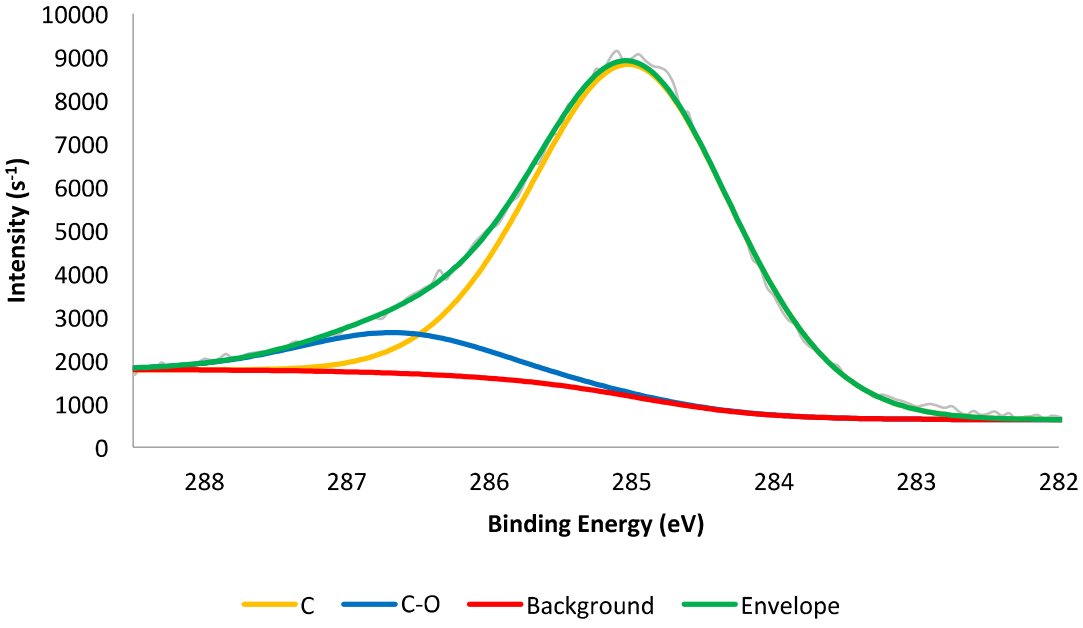
10000
9000
8000
7000
6000
5000
4000
3000
2000
1000
0
Intensity (s-1)
288
287
286
285
284
283
282
Binding Energy (eV)
C
C-O
Background
Envelope

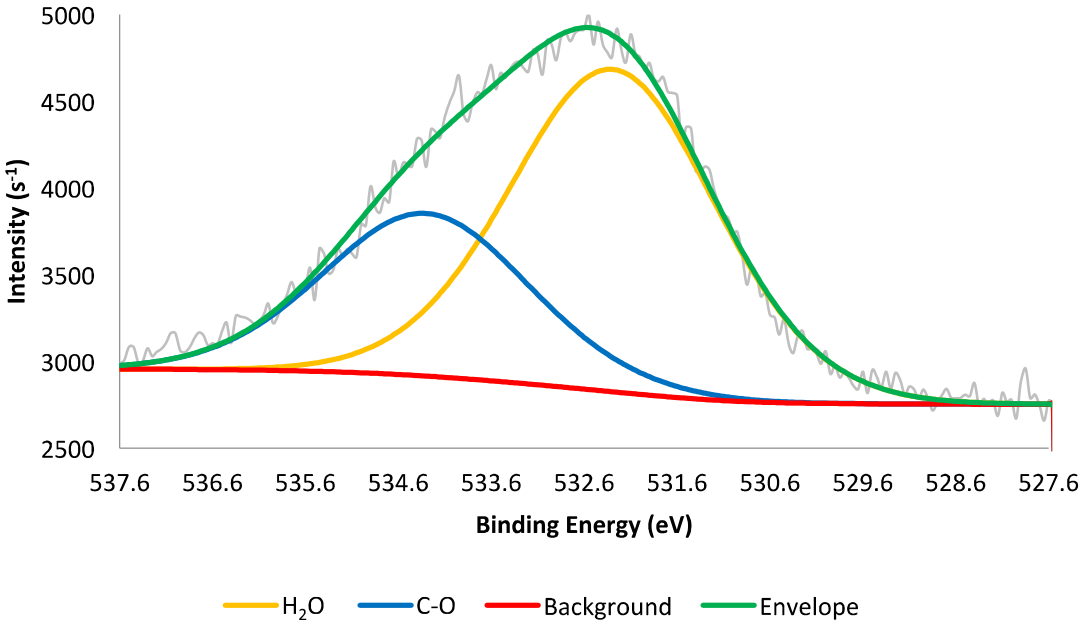
5000
4500
4000
3500
3000
2500
Intensity (s-1)
537.6
536.6
535.6
534.6
533.6
532.6
531.6
530.6
529.6
528.6
527.6
Binding Energy (eV)
H2O
C-O
Background
Envelope

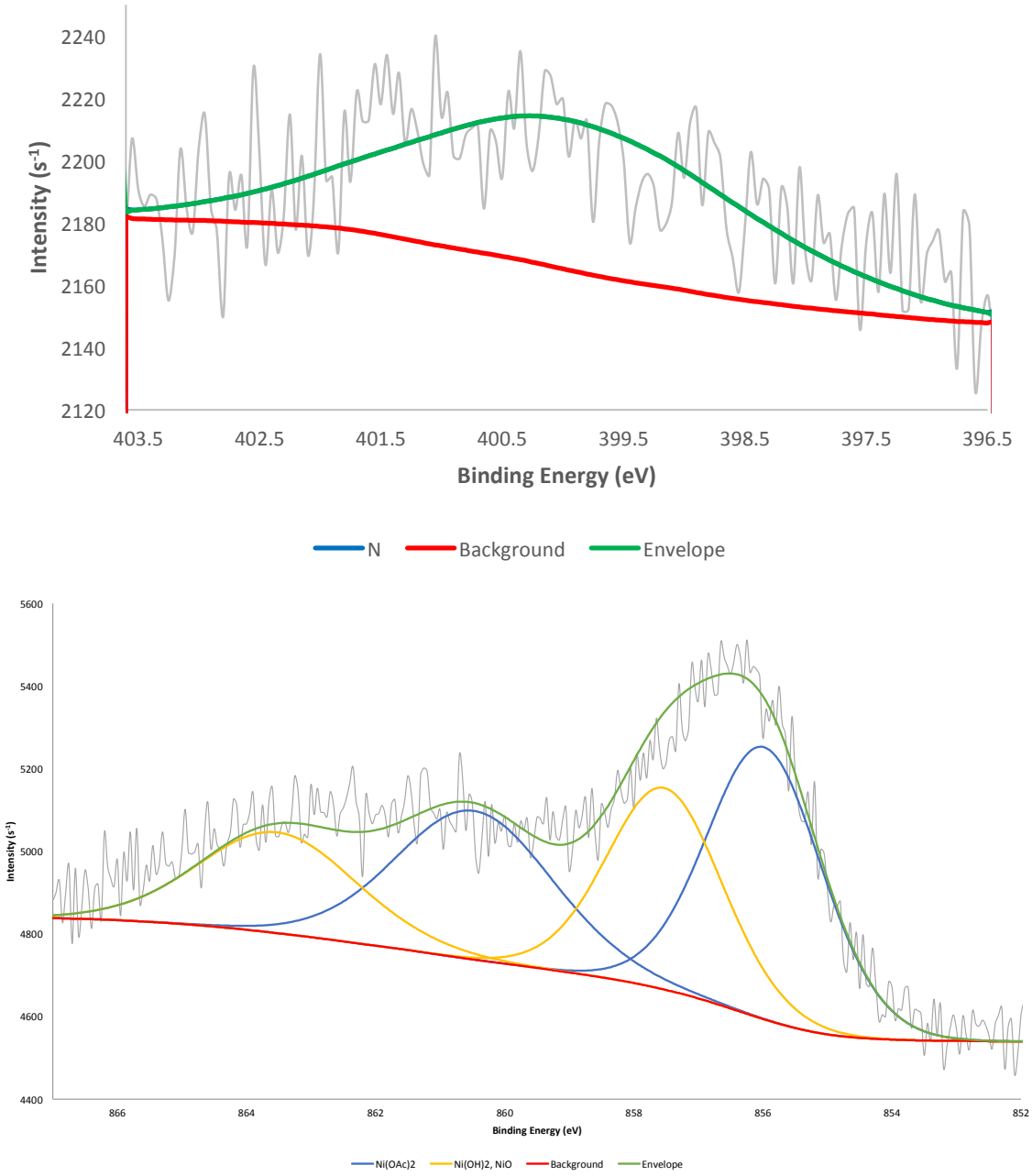

Figure S4. X-ray photoelectron spectra of the Ni-doped biochar. From top to bottom: C1s, O1s, N1s, and Ni2p$_{3/2}$.

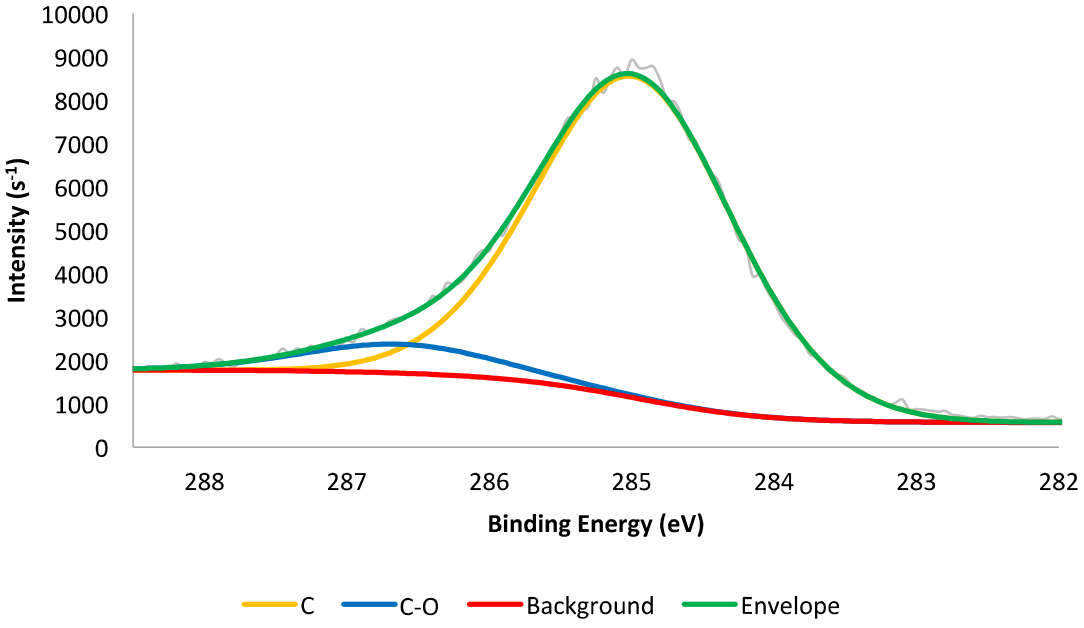
10000
9000
8000
7000
6000
5000
4000
3000
2000
1000
0
Intensity (s-1)
288
287
286
285
284
283
282
Binding Energy (eV)
C
C-O
Background
Envelope

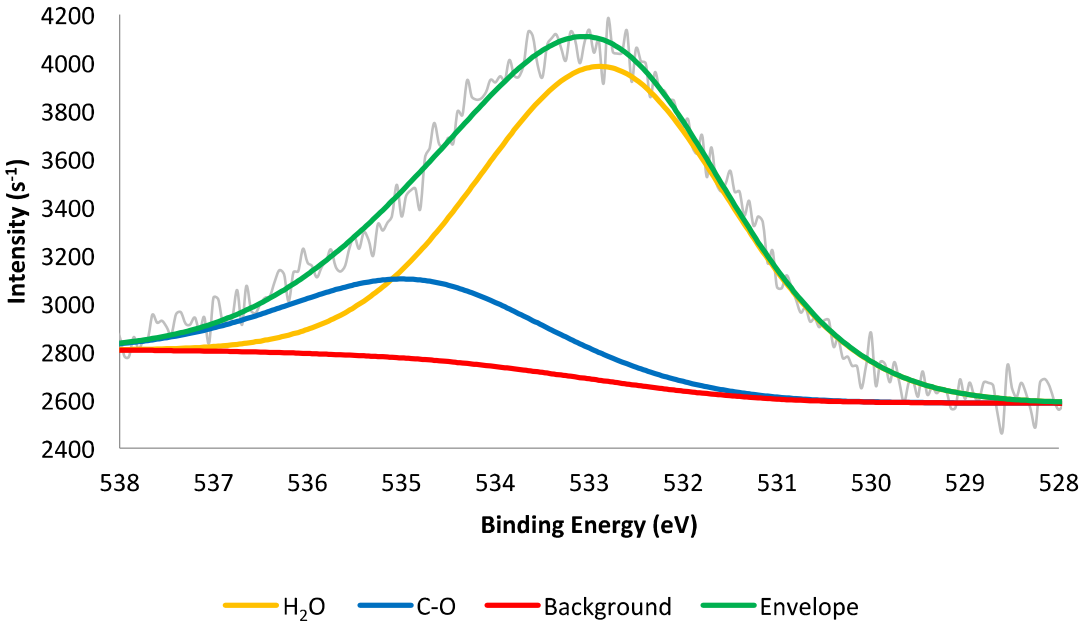
4200
4000
3800
3600
3400
3200
3000
2800
2600
2400
Intensity (s-1)
538
537
536
535
534
533
532
531
530
529
528
Binding Energy (eV)
H2O
C-O
Background
Envelope

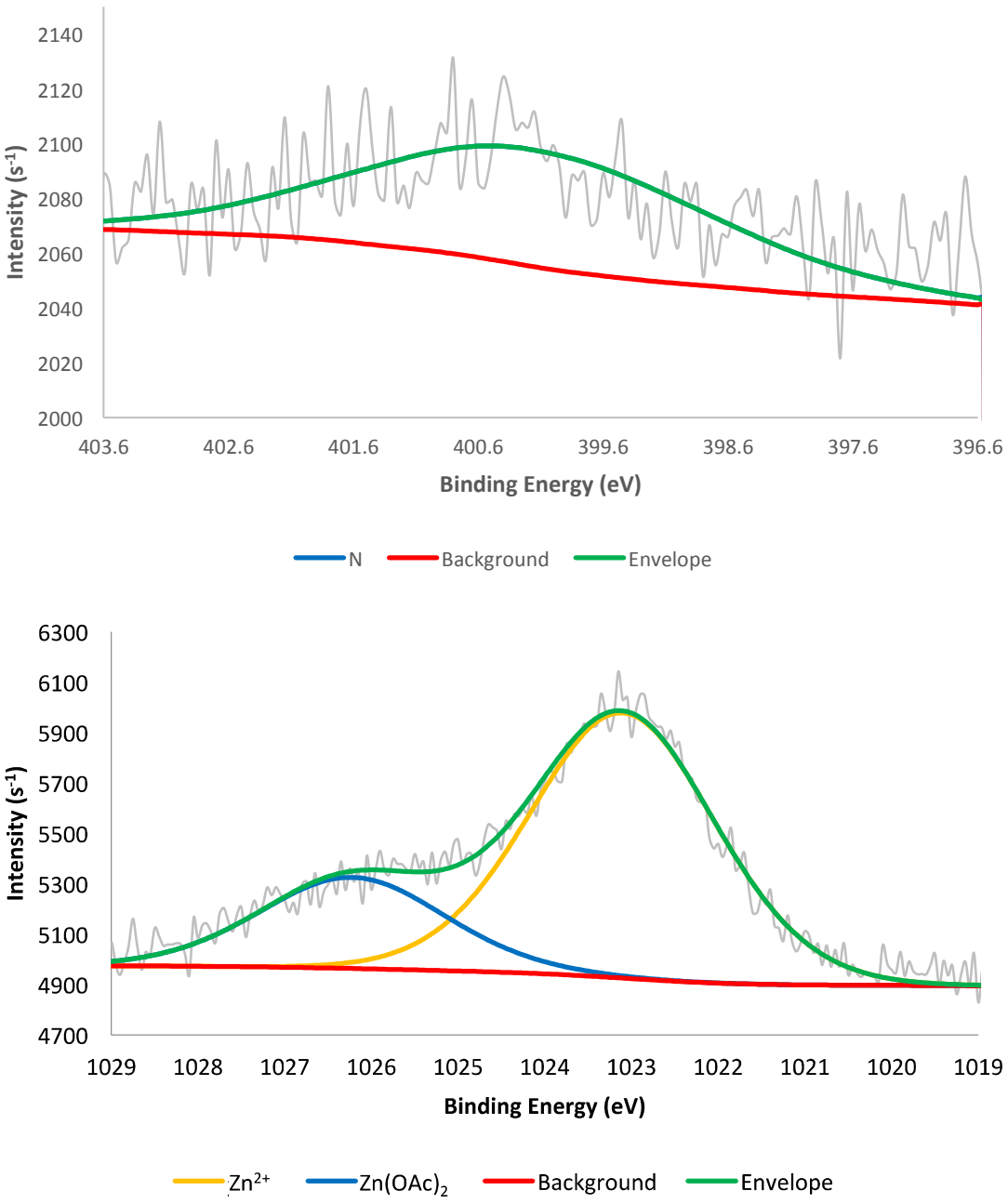

Figure S5. X-ray photoelectron spectra of the Zn-doped biochar. From top to bottom: C1s, O1s, N1s, and $Zn2p_{3/2}$.

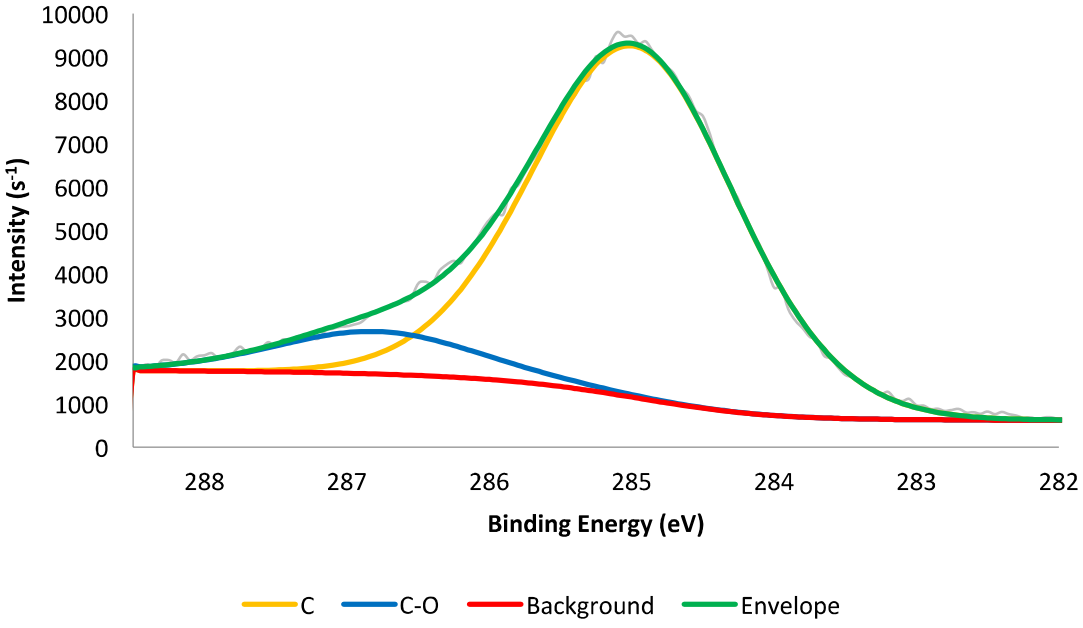
10000
9000
8000
7000
6000
5000
4000
3000
2000
1000
0
Intensity (s-1)
288
287
286
285
284
283
282
Binding Energy (eV)
C
C-O
Background
Envelope

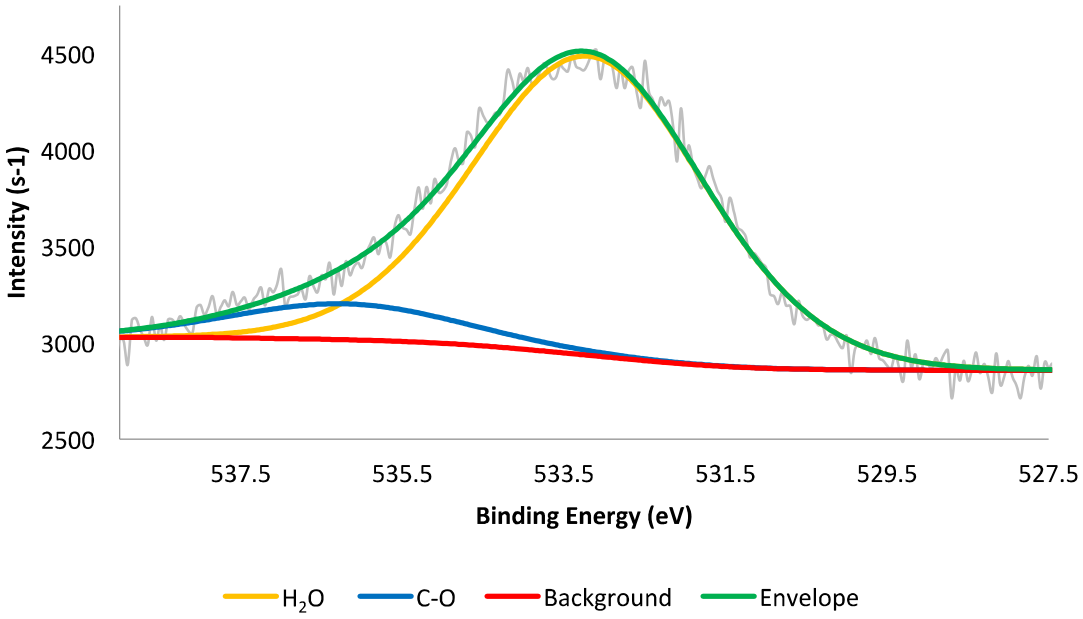
4500
4000
3500
3000
2500
Intensity (s-1)
537.5
535.5
533.5
531.5
529.5
527.5
Binding Energy (eV)
H2O
C-O
Background
Envelope

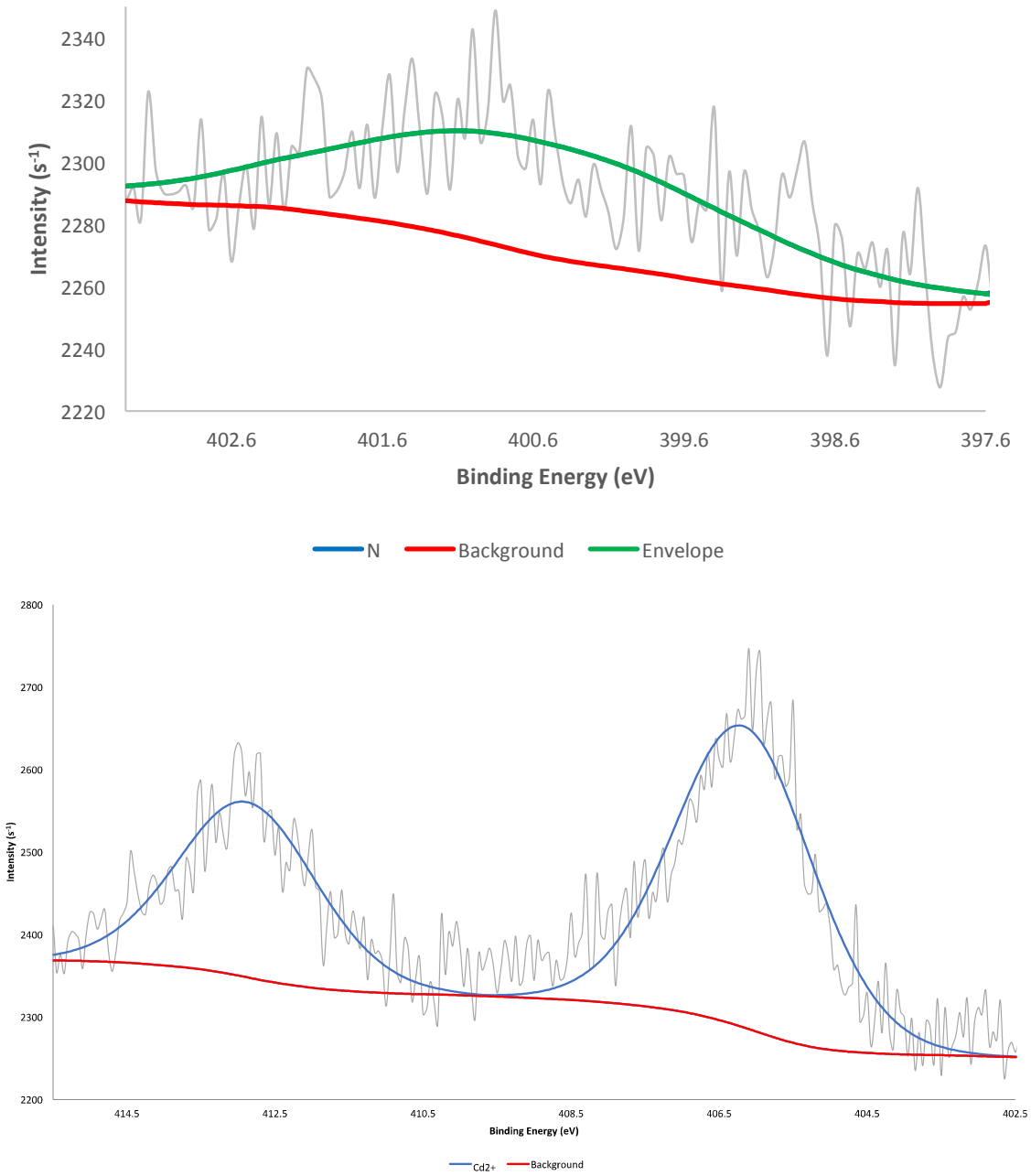

Figure S6. X-ray photoelectron spectra of the Cd-doped biochar. From top to bottom: C1s, O1s, N1s, and $Cd3d_{5/2}$.

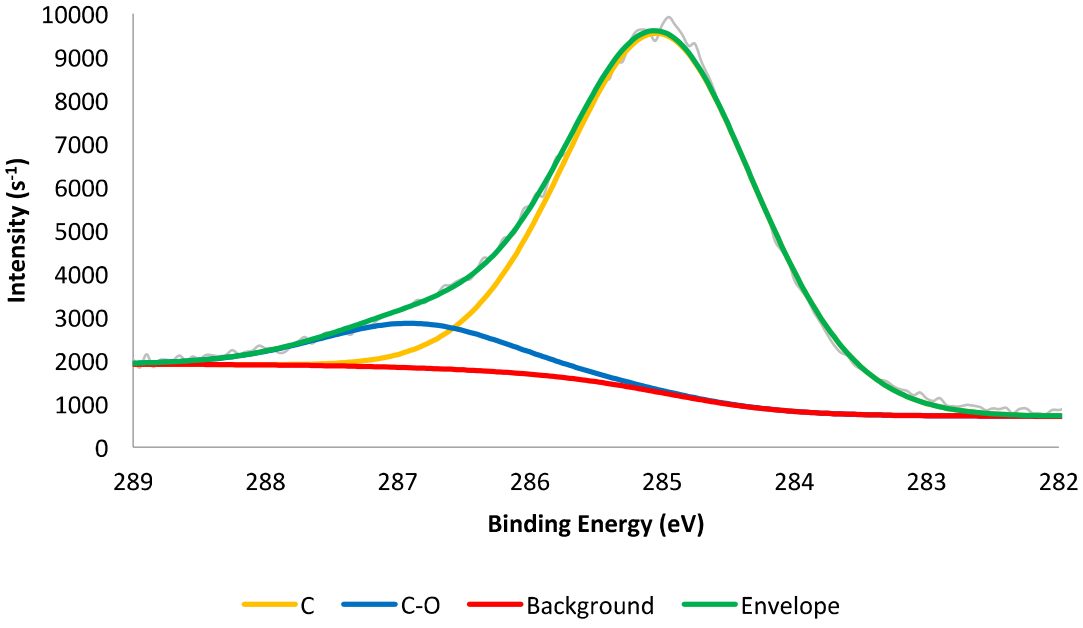
10000
9000
8000
7000
6000
5000
4000
3000
2000
1000
0
Intensity (s-1)
289
288
287
286
285
284
283
282
Binding Energy (eV)
C
C-O
Background
Envelope

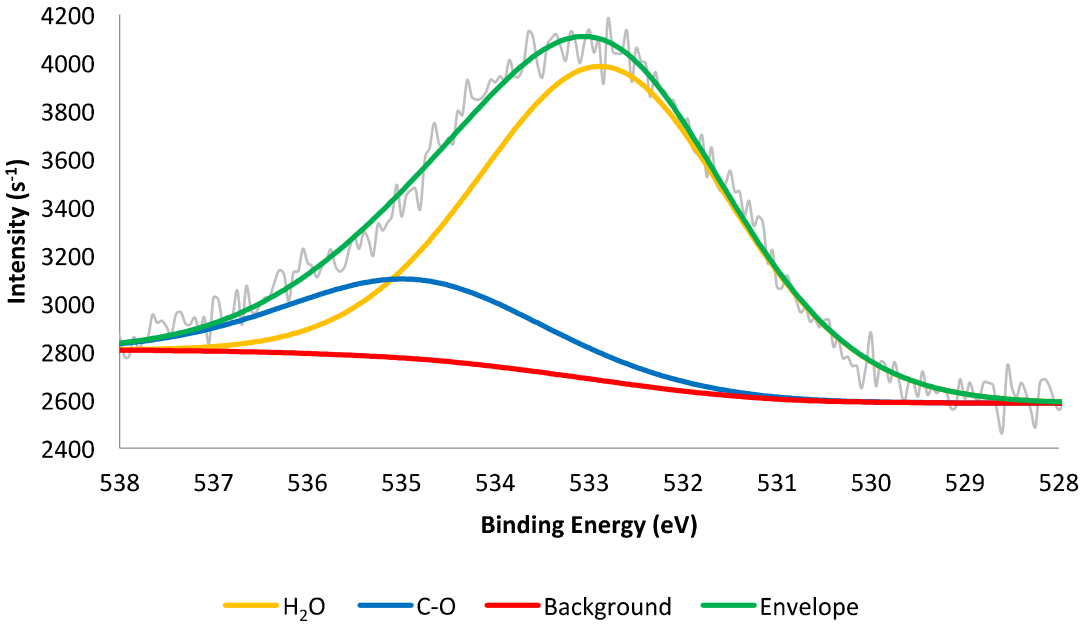
4200
4000
3800
3600
3400
3200
3000
2800
2600
2400
Intensity (s-1)
538
537
536
535
534
533
532
531
530
529
528
Binding Energy (eV)
H2O
C-O
Background
Envelope

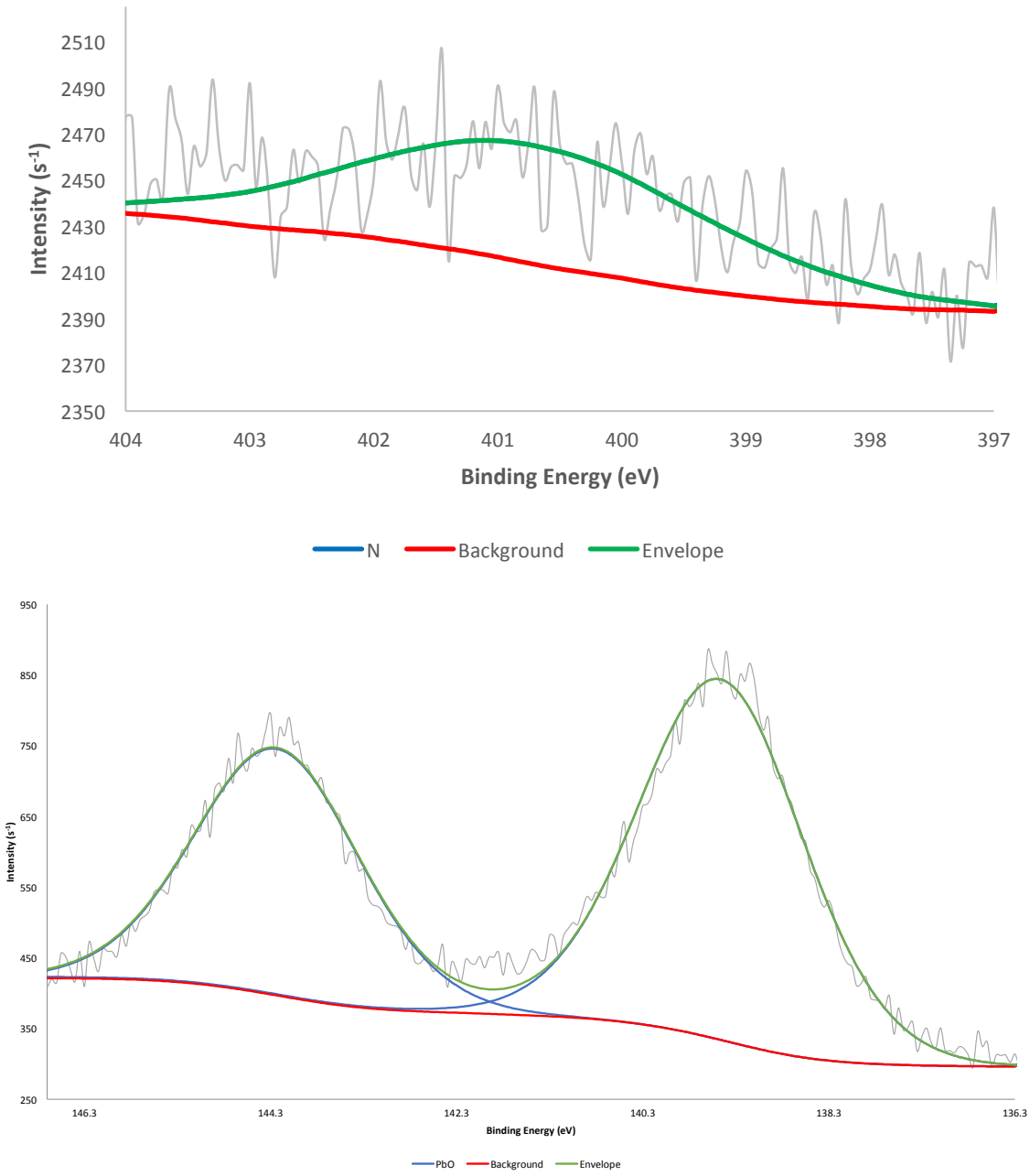

Figure S7. X-ray photoelectron spectra of the Pb-doped biochar. From top to bottom: C1s, O1s, N1s, and Pb4f$_{5/2}$ and Pb4f$_{7/2}$.

Table S1. X-ray photoelectron binding energies for metal-ion doped biochar.

Biochar	Peak	Binding Energy (eV)	Relative area
Mn^{2+}	C1s	285.0	1
	C1s	286.7	0.16
	O1s	532.9	1
	O1s	534.3	0.42
	N1s	400.3	1
	$Mn2p_{3/2}$	642.7	1
	$Mn2p_{3/2}$	647.1	0.52
Cu^{2+}	C1s	285.0	1
	C1s	286.7	0.17
	O1s	532.8	1
	O1s	534.4	0.42
	N1s	400.1	1
	$Cu2p_{3/2}$	935.0	1
	$Cu2p_{3/2}$	939.2	0.39
	$Cu2p_{3/2}$	944.1	0.48
Ni^{2+}	C1s	285.0	1
	C1s	286.6	0.12
	O1s	532.3	1
	O1s	534.3	0.5
	N1s	399.9	1
	$Ni2p_{3/2}$	856.5	1
	$Ni2p_{3/2}$	860.7	0.44
	$Ni2p_{3/2}$	863.8	0.34
Zn^{2+}	C1s	285.0	1
	C1s	286.6	0.09
	O1s	532.8	1
	O1s	534.9	0.25
	N1s	400.2	1
	$Zn2p_{3/2}$	1023.1	1
	$Zn2p_{3/2}$	1026.2	0.34
Cd^{2+}	C1s	285.0	1
	C1s	286.8	0.12
	O1s	533.2	1
	O1s	536.2	0.12
	N1s	400.6	1
	$Cd3d_{5/2}$	406.2	1
Cd^{2+}	$Cd3d_{5/2}$	412.9	0.58
Pb^{2+}	C1s	285.0	1
	C1s	286.9	0.12
	O1s	532.9	1
	O1s	534.7	0.23
	N1s	400.7	1

	$Pb4f_{7/2}$	139.5	1
	$Pb4f_{5/2}$	144.2	0.68

Table S2. Equilibrium adsorption data for birch biochar.[a]

M^{n+}	C_0 (mg L^{-1})	C_e (mg L^{-1})	m (mg)	q_e (mg g^{-1})[b]	% removal
Mn^{2+}	62.9±0.6	49.9±0.2	97.3	0.67±0.03	20.7
	119.3±0.6	105.5±0.6	96.7	0.71±0.04	11.6
	173.3±1.2	157.2±0.6	93.6	0.86±0.07	9.3
	236.2±0.5	213.4±1.1	98.1	1.16±0.06	9.7
Cu^{2+}	63.5±0.1	13.5±0.1	102.5	2.44±0.01	78.7
	107.8±0.1	51.9±0.1	103.8	2.69±0.01	51.9
	191±0.8	125.6±0.3	98.7	3.31±0.04	34.2
	224±0.4	159.1±0.3	107.2	3.03±0.03	29.0
Ni^{2+}	59±1.1	39.7±1.2	100.0	0.97±0.08	32.7
	95.2±0.7	66.5±1.1	101.8	1.41±0.06	30.1
	166.1±1	132.3±0.5	103.4	1.63±0.05	20.3
	203.3±1	168.2±1.2	95.4	1.84±0.08	17.3
Zn^{2+}	61.3±0.5	14.0±0	96.0	5.17±0.08	77.2
	120.8±1.9	61.8±1	103.3	5.57±0.16	48.8
	195.9±3.5	115.8±1.9	98.0	6.8±0.25	40.9
	238.3±2.9	161.2±2.1	100.0	6.57±0.23	32.4
Cd^{2+}	55±0.3	12.8±0.2	96.1	2.2±0.02	76.7
	122.1±0.4	57.9±0.1	98.0	3.28±0.02	52.6
	195.2±1	90.5±0.4	97.6	5.36±0.05	53.6
	257.6±1	141.5±0.3	98.7	5.88±0.05	45.1
Pb^{2+}	51.4±0.4	N/D	101.7	2.53±0.02	>99.9
	111.8±0.4	N/D	94.2	5.93±0.02	>99.9
	156.6±1.3	N/D	107.1	7.31±0.06	>99.9
	192.2±1.7	N/D	94.1	10.21±0.09	>99.9
	55.6±0.5	16.2±0.4	16.4	12.01±0.19	70.9
	116.1±0.3	62.6±0.5	17.7	15.11±0.17	46.1
	161±0.8	106.3±0.3	18.5	14.78±0.23	34.0
	204±1	138.4±1.1	18.8	17.45±0.4	32.2

[a]Reported errors correspond to 1σ for n=3 measurements. N/D, not detected.
[b]Endogenous metal ions are included for Zn^{2+}.

Table S3. Equilibrium adsorption data for Norit activated carbon.

M^{n+}	C_0 (mg L^{-1})	C_e (mg L^{-1})	m (mg)	q_e (mg g^{-1})	% removal
Mn^{2+}	62.9±0.6	62.4±1	96.9	0.03±0.06	0.8
	119.3±0.6	113.4±0.9	98.2	0.30±0.06	4.9
	173.3±1.2	165.5±0.5	101.9	0.38±0.06	4.5
	236.2±0.5	231.6±0.9	103.5	0.22±0.05	1.9
Cu^{2+}	63.5±0.1	53.1±0.3	102.8	0.51±0.01	16.4
	107.8±0.1	98.3±0.4	97.2	0.49±0.02	8.8
	191±0.8	175.5±1.6	106.3	0.73±0.08	8.1
	224±0.4	208.1±2.3	107.9	0.74±0.11	7.1
Ni^{2+}	59±1.1	60.1±0.4	102.4	-0.05±0.06	~0
	95.2±0.7	90.1±0.5	105.9	0.24±0.04	5.4
	166.1±1	170.4±0.3	104.4	-0.21±0.05	~0
	203.3±1	201.2±1	103.3	0.10±0.07	1.0
Zn^{2+}	61.3±0.5	64.2±0.6	101.5	-0.14±0.04	~0
	120.8±1.9	127.1±2.3	93.0	-0.34±0.16	~0
	195.9±3.5	188.7±1.3	100.9	0.36±0.19	3.7
	238.3±2.9	247.7±1.7	108.9	-0.43±0.15	~0
Cd^{2+}	55±0.3	54.2±0.3	100.6	0.04±0.02	1.5
	122.1±0.4	118.4±0.6	95.8	0.19±0.04	3.0
	195.2±1	191±1.3	93.5	0.22±0.09	2.2
	257.6±1	257.6±1	95.5	0±0.08	0
Pb^{2+}	51.4±0.4	36.3±0.5	92.3	0.82±0.03	29.4
	111.8±0.4	86.4±0.3	97.6	1.30±0.03	22.7
	156.6±1.3	121.6±0.2	110.8	1.58±0.06	22.3
	192.2±1.7	150.8±0.3	98.2	2.11±0.09	21.5

[a]Reported errors correspond to 1σ for n=3 measurements. N/D, not detected.

Table S4. Equilibrium adsorption data for acid-washed birch biochar.

M^{n+}	C_e (mg L^{-1})	m (mg)	q_e (mg g^{-1})	% removal
Mn^{2+}	244.2±2.4	0		
	243.4±1	24.3	0.16±0.68	0.3
	236.2±0.7	54.5	0.73±0.29	3.3
	239.7±1	70.6	0.32±0.24	1.8
	239.9±1.2	104.5	0.21±0.18	1.8
	239.5±1.2	192.8	0.12±0.09	1.9
Cu^{2+}	237.9±0.7	0		
	237±0.9	27.1	0.17±0.31	0.4
	235.3±0.7	47.0	0.28±0.15	1.1
	231.7±0.7	75.9	0.41±0.09	2.6
	229.9±1.1	100.8	0.4±0.09	3.4
	218.1±0.9	190.6	0.52±0.04	8.3
Ni^{2+}	196.3±0.4	0		
	198.3±0.6	24.8	-0.4±0.2	~0
	201.5±1	59.8	-0.43±0.12	~0
	200.2±0.8	75.9	-0.26±0.08	~0
	195.2±0.6	101.3	0.05±0.04	0.6
	196.7±1	196.3	-0.01±0.03	~0
Zn^{2+}	238.9±1.7	0		
	250±1	23.1	-2.4±0.58	~0
	248.2±1.2	55.0	-0.85±0.27	~0
	240±0.7	76.0	-0.07±0.15	~0
	244.6±1	105.4	-0.27±0.13	~0
	251.1±1.8	196.6	-0.31±0.09	~0
Cd^{2+}	247.2±0.2	0		
	241.1±1	25.9	1.18±0.23	2.5
	238.1±0.5	42.5	1.07±0.09	3.7
	233.9±0.5	71.8	0.93±0.05	5.4
	240.9±1	101.2	0.31±0.06	2.5
	238±0.2	199.6	0.23±0.01	3.7
Pb^{2+}	212.8±0.9	0		
	216.6±1.3	3.8	-5±2.83	~0
	224.2±1.8	8.5	-6.71±1.56	~0
	214.7±1.1	23.1	-0.41±0.42	~0
	219.4±1.3	49.8	-0.66±0.22	~0
	209.4±0.8	72.8	0.23±0.11	1.6
	203.7±1.2	108.9	0.42±0.1	4.3

[a]Reported errors correspond to 1σ for n=5 measurements.

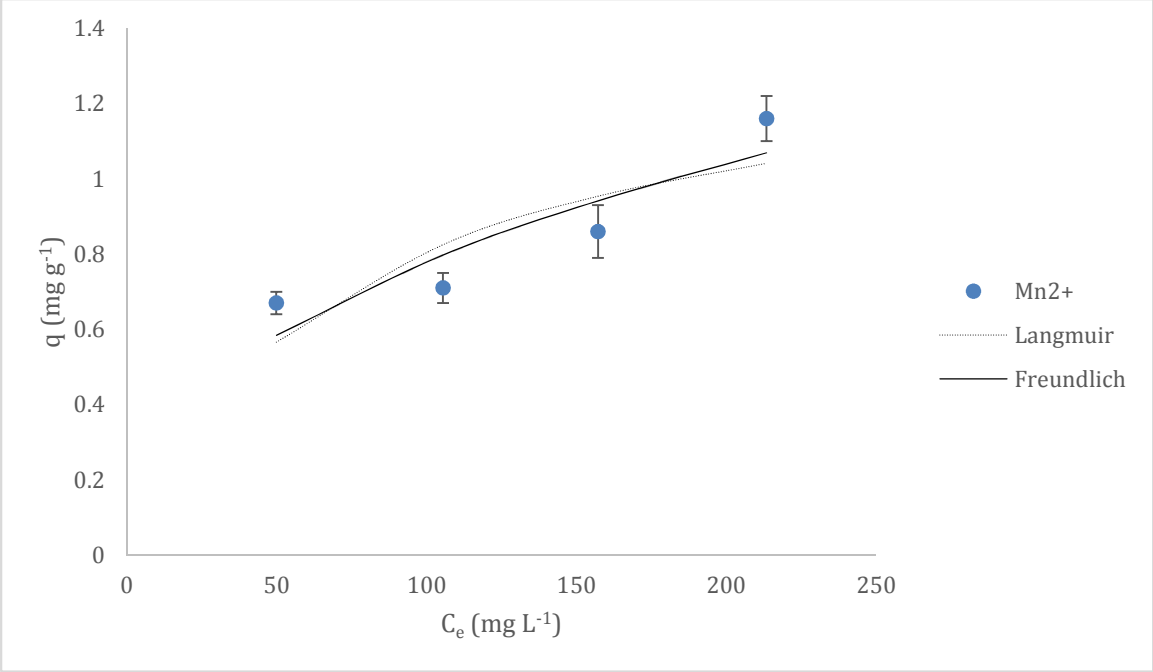

Figure S8. Mn^{2+} adsorption isotherm plots on birch biochar.

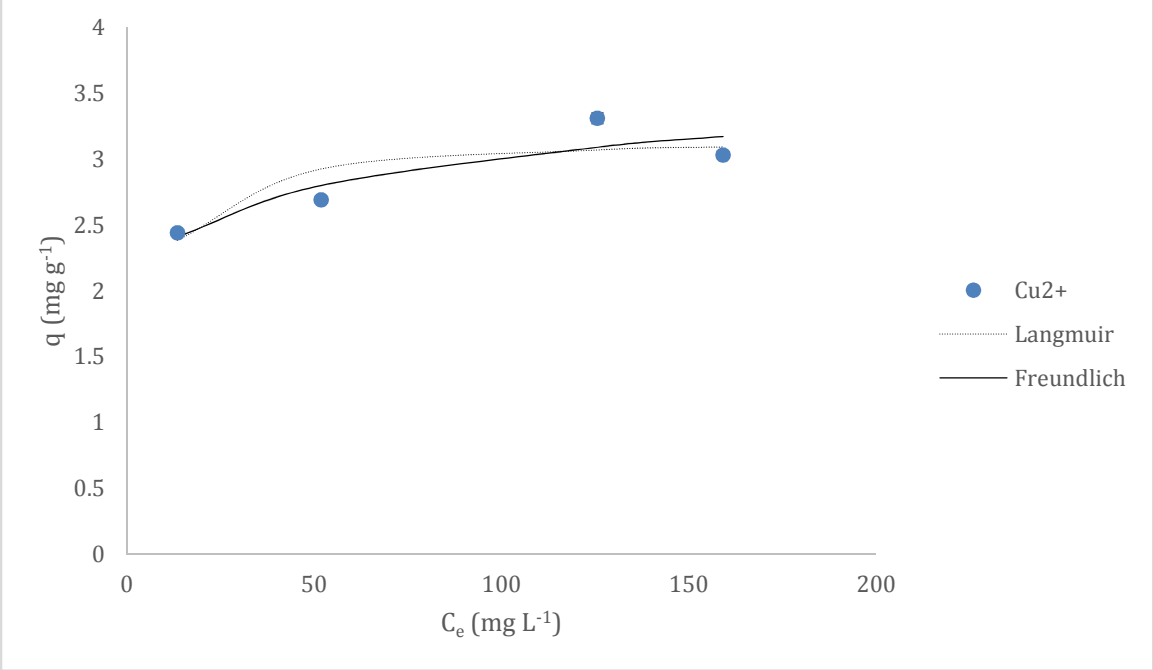

Figure S9. Cu^{2+} adsorption isotherm plots on birch biochar.

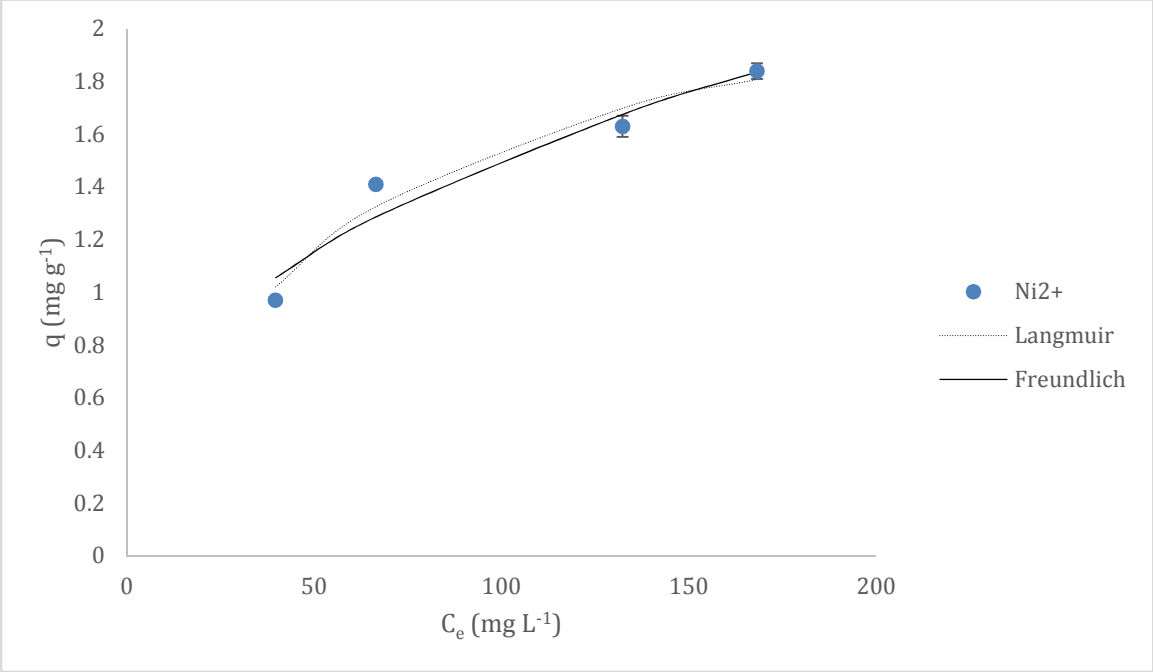

Figure S10. Ni^{2+} adsorption isotherm plots on birch biochar.

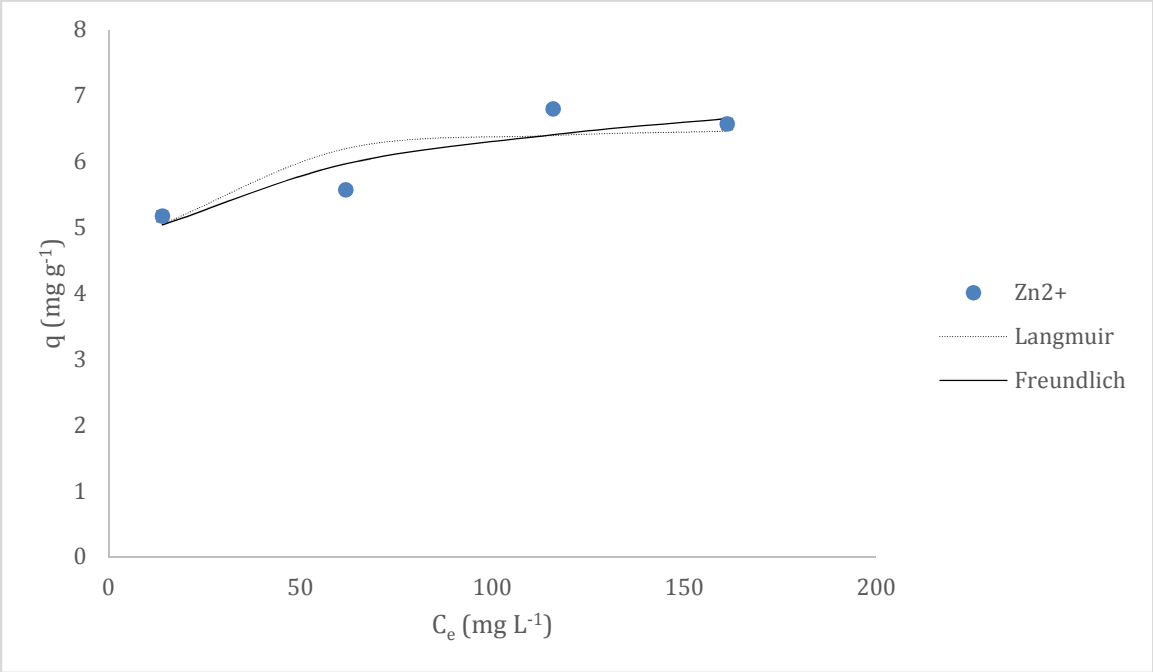

Figure S11. Zn^{2+} adsorption isotherm plots on birch biochar.

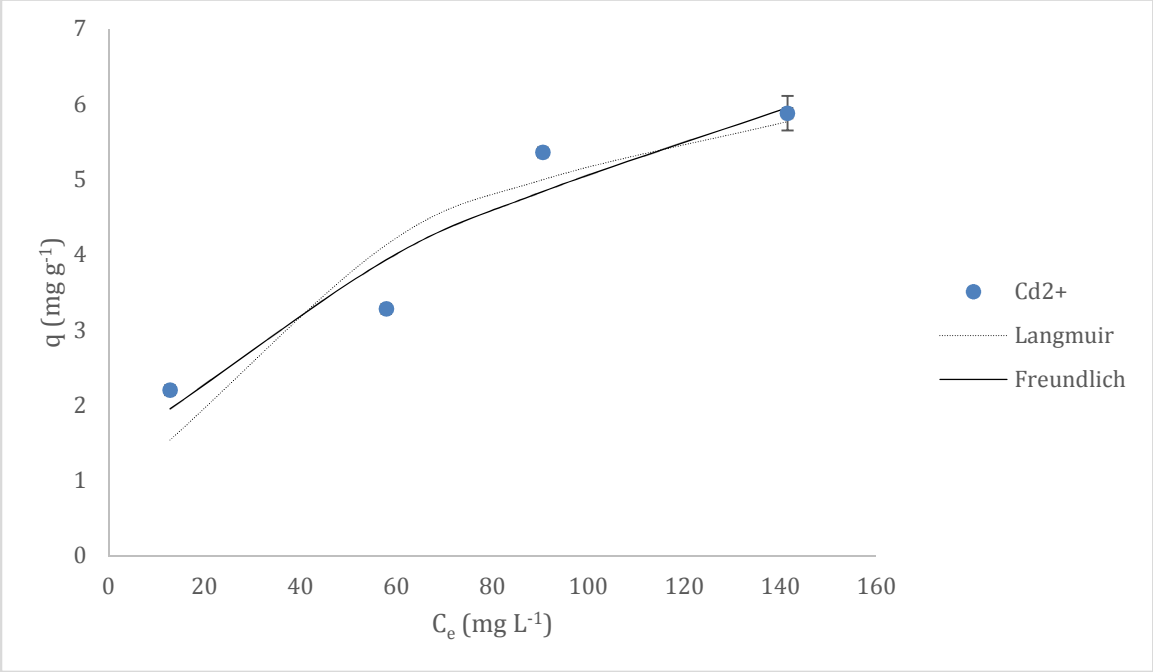

Figure S12. Cd^{2+} adsorption isotherm plots on birch biochar.

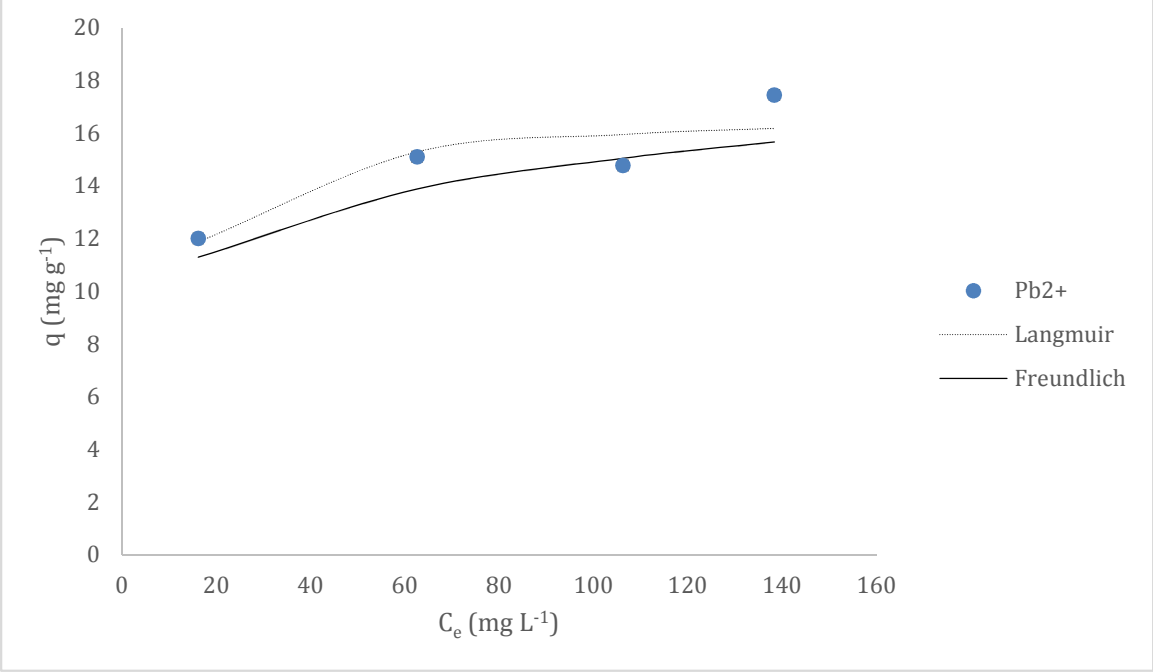

Figure S13. Pb^{2+} adsorption isotherm plots on birch biochar.

Table S5. Freundlich isotherm model constants for metal ion adsorption on birch biochar.[a]

M^{n+}	n	K	RMSE
Mn^{2+}	2.4±1.10	0.12	0.086
Cu^{2+}	8.9±2.82	1.8	0.14
Ni^{2+}	2.6±0.46	0.26±0.15	0.07
Zn^{2+}	8.78±2.96	3.73±0.07	0.28
Cd^{2+}	2.15±0.50	0.60±0.16	0.44
Pb^{2+}	6.54±1.79	7.38±0.07	1.14

[a]n, adsorption intensity; K_L, adsorption capacity; and RMSE, root mean square error. Reported errors correspond to 1σ for n=3 measurements.

Table S6. Langmuir isotherm constants for metal ion adsorption onto Norit activated carbon.[a]

M^{n+}	q_m (mg g^{-1})	K_L (g L^{-1})	R^2
Mn^{2+}	-0.21±0.29	$-2.89\pm4.50\times10^{-3}$	0.199
Cu^{2+}	0.97±0.20	$1.48\pm0.75\times10^{-2}$	0.919
Ni^{2+}	0.07±0.06	$-8.1\pm10.9\times10^{-3}$	0.390
Zn^{2+}	1.04±4.81	$-2.6\pm13.1\times10^{-3}$	0.023
Cd^{2+}	-0.29±0.37	$-2.50\pm3.29\times10^{-3}$	0.392
Pb^{2+}	3.86±1.40	$6.61\pm2.93\times10^{-2}$	0.792

[a]Reported errors correspond to 1σ for n=3 measurements.

Table S7. Freundlich isotherm constants for metal ion adsorption onto Norit activated carbon.[a]

M^{n+}	n	log K_F	R^2
Mn^{2+}	0.62±0.34	-4.20±1.92	0.616
Cu^{2+}	3.16±1.22	-0.87±0.25	0.770
Ni^{2+b}	-0.92	1.51	1
Zn^{2+c}	N/A	N/A	N/A
Cd^{2+}	0.71±0.22	-3.8±0.92	0.908
Pb^{2+}	1.61±0.21	-1.07±0.16	0.967

[a]Reported errors correspond to 1σ for n=3 measurements. [b]Only two data points were available. [c]Only one data point was available

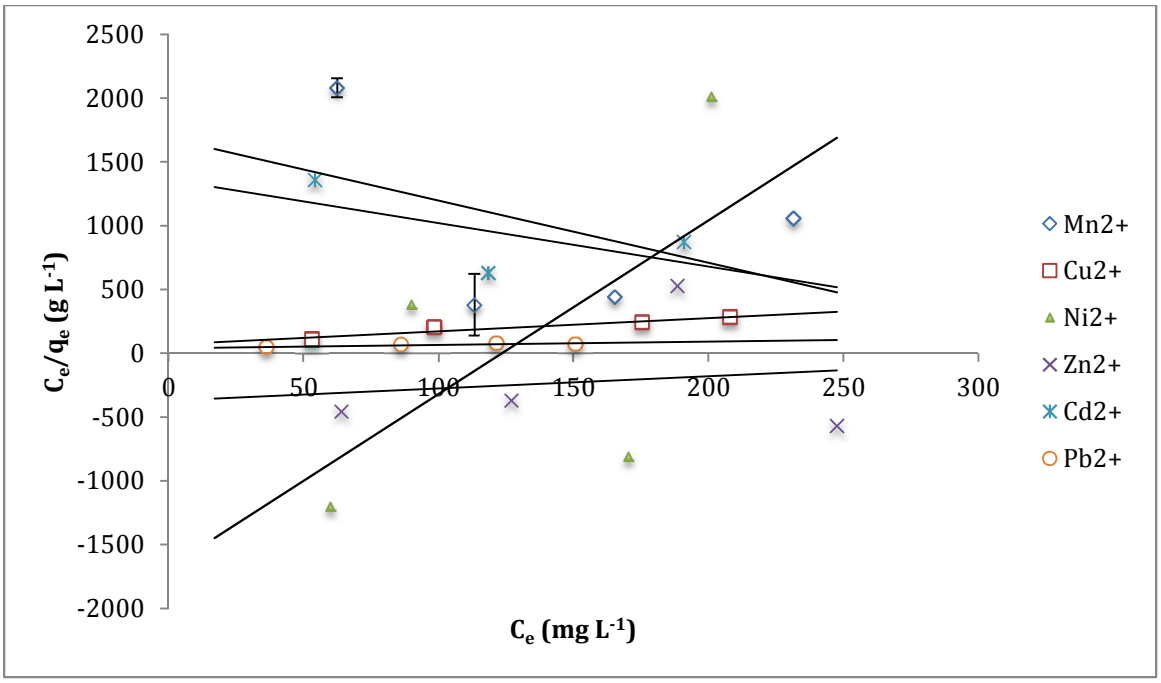

Figure S14. Linearized Langmuir plots for Norit activated carbon. Error bars correspond to 1σ for n=3 measurements.

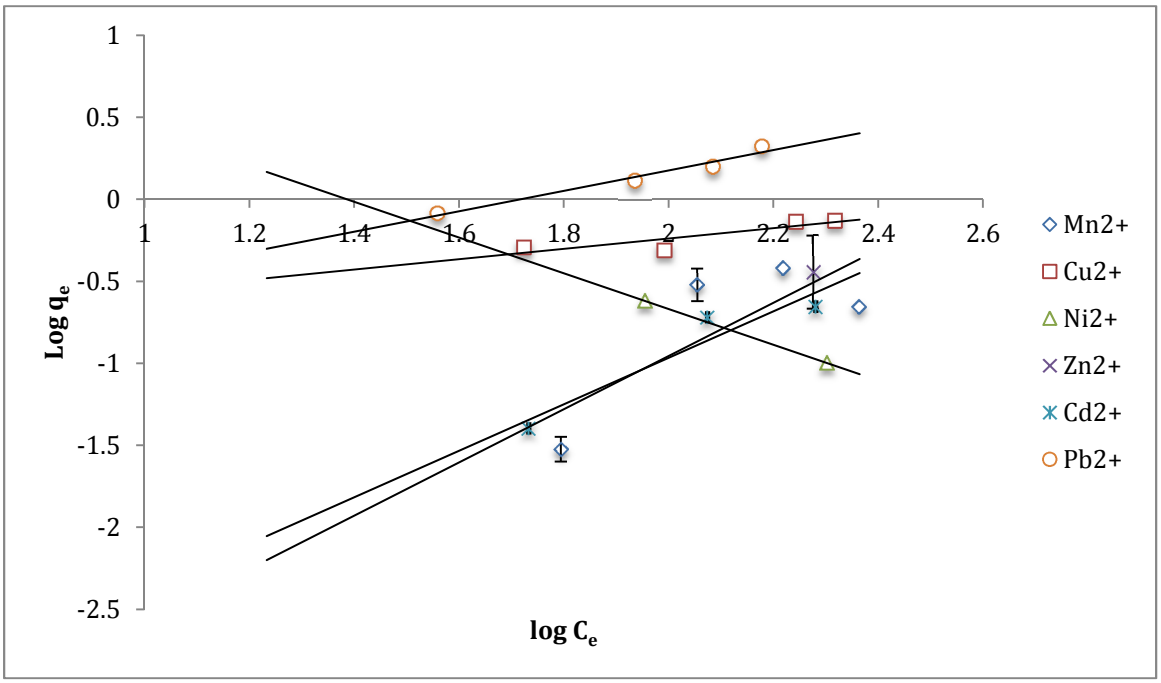

Figure S15. Linearized Freundlich plots for Norit activated carbon. Error bars correspond to 1σ for n=3 measurements.

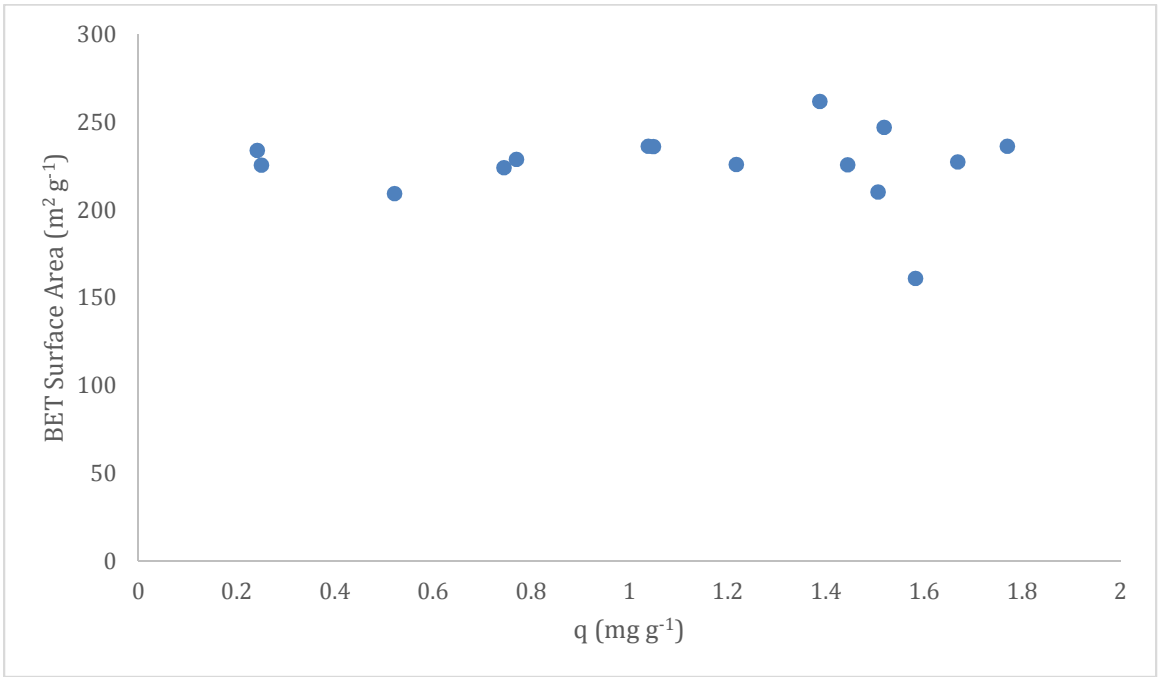

Figure S16. Biochar BET surface area as a function of Cu^{2+} loading.

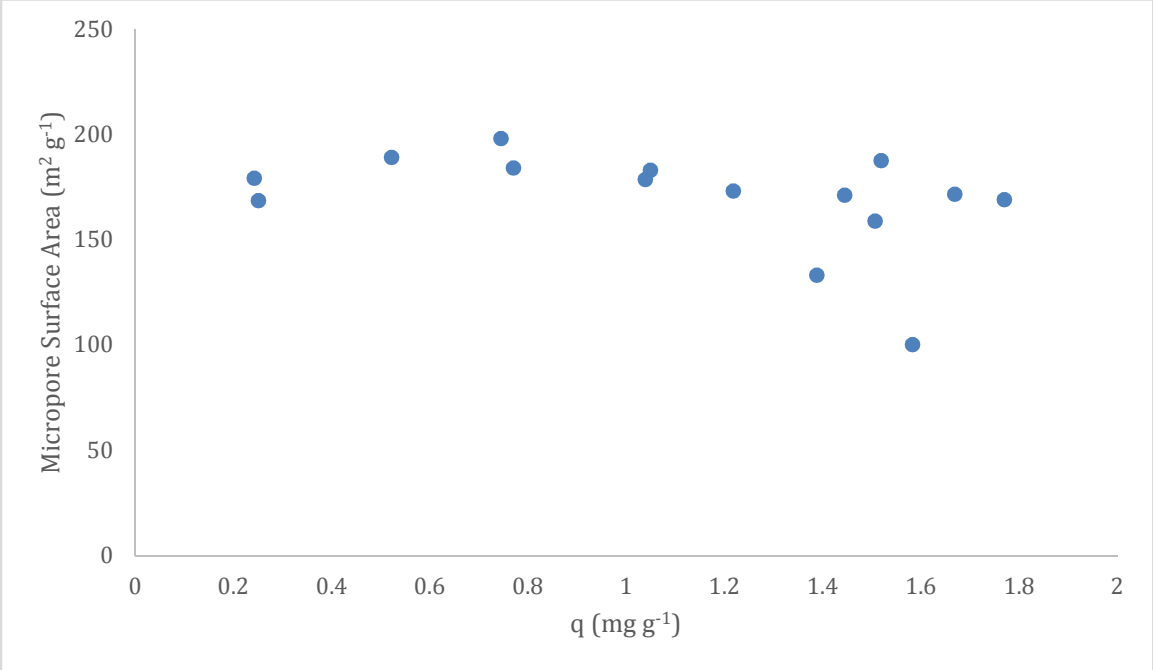

Figure S17. Biochar micropore surface area as a function of Cu^{2+} loading.

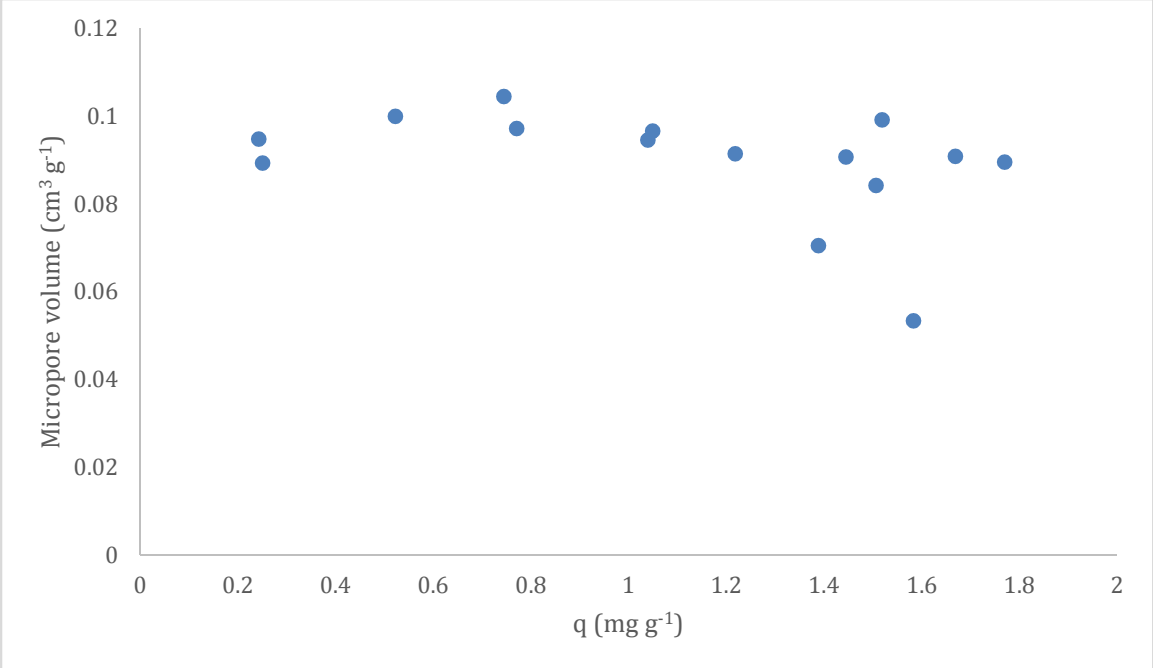

Figure S18. Biochar micropore volume as a function of Cu^{2+} loading.

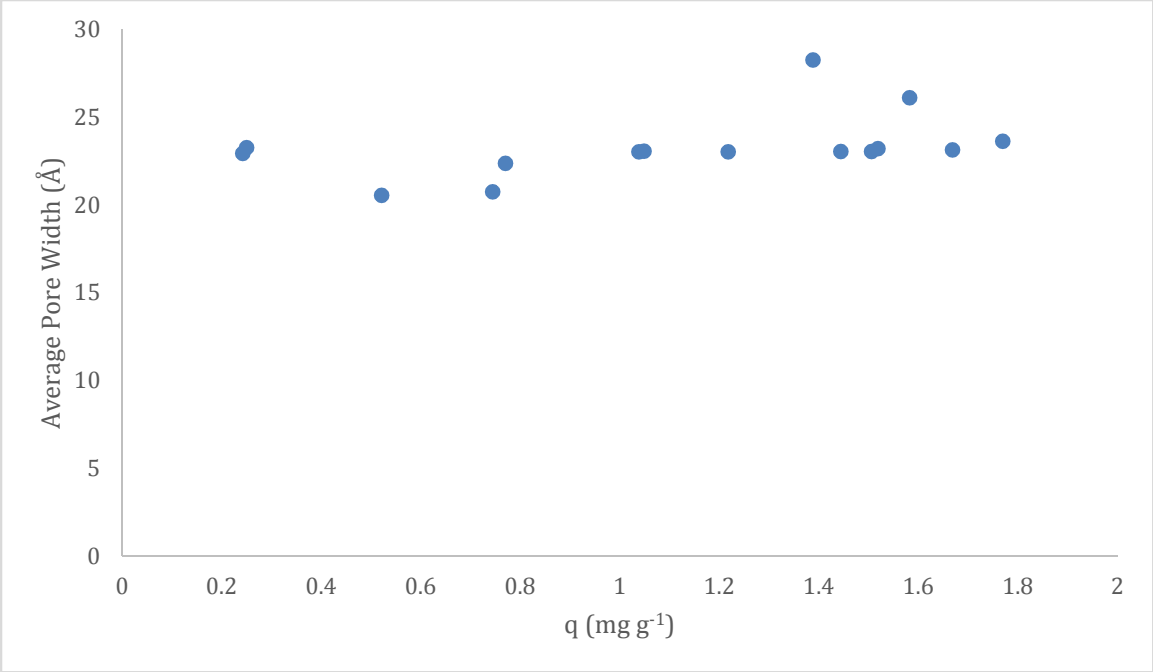

Figure S19. Biochar average pore width as a function of Cu^{2+} loading.

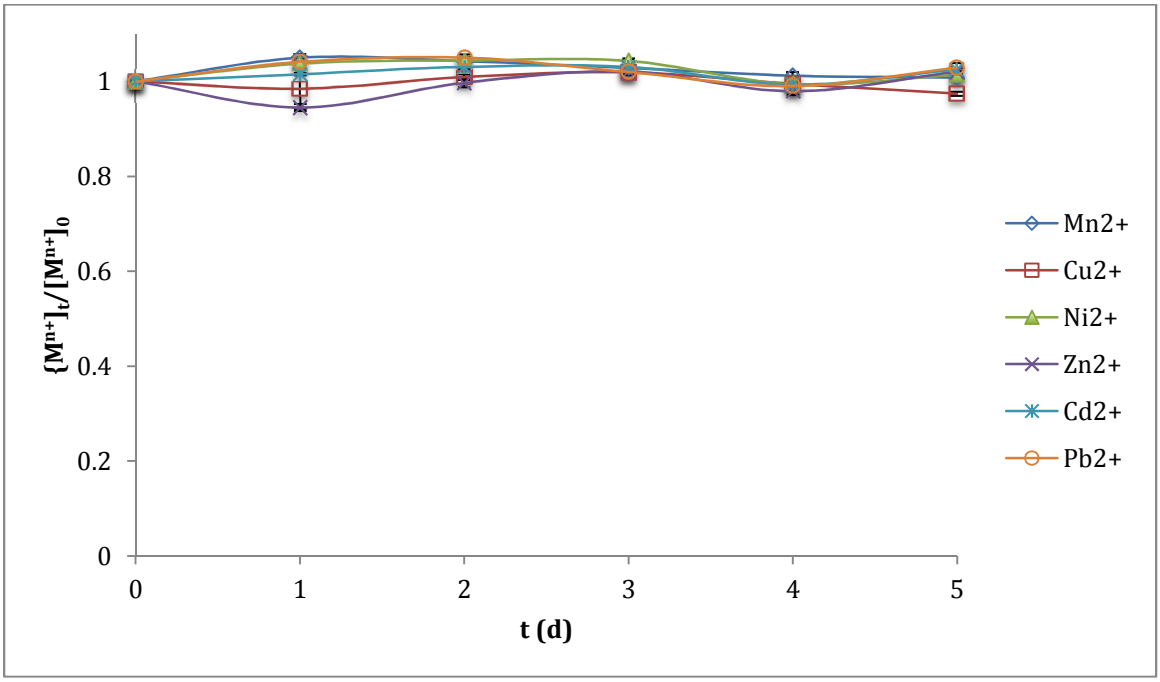

Figure S20. Kinetics of adsorption onto acid-washed biochar. Error bars correspond to 1σ for n=5 measurements.